9. Steinbach, A. H., Martinis, J. M. & Devoret, M. H. Observation of hot-electron shot noise in a metallic resistor. *Phys. Rev. Lett.* **76,** 3806–3809 (1996).
10. Henny, M., Oberholzer, S., Strunk, C. & Schönenberger, C. 1/3-shot-noise supression in diffusive nanowires. *Phys. Rev. B* **59,** 2871–2880 (1999).
11. Blanter, Ya. M. & Büttiker, M. Shot noise in mesoscopic conductors. Preprint condmat/9910158 at ⟨http://xxx.lanl.gov⟩ (1999).
12. Andreev, A. F. The thermal conductivity of the intermediate state in superconductors. *Sov. Phys. JETP* **19,** 1228–1231 (1964).
13. Muzykantskii, B. A. & Khmelnitskii, D. E. Quantum shot noise in a normal-metal-superconductor point contact. *Phys. Rev. B* **50,** 3982–3987 (1994).
14. Dieleman, P., Bukkems, H. G., Klapwijk, T. M., Schicke, M. & Gundlach, K. H. Observation of Andreev reflection enhanced shot noise. *Phys. Rev. Lett.* **79,** 3486–3489 (1997).
15. Hoss, T. *et al.* Multiple Andreev reflection and giant excess noise in diffusive superconductor/normal-metal/superconductor junctions. Preprint cond-mat 9901129 at ⟨http://xxx.lanl.gov⟩ (1999).
16. Jehl, X., Payet-Burin, P., Baraduc, C., Calemczuk, R. & Sanquer, M. Andreev reflection enhanced shot noise in mesoscopic SNS junctions. *Phys. Rev. Lett.* **83,** 1660–1663 (1999).
17. Nagaev, K. E. Influence of electron-electron scattering on shot noise in diffusive contacts. *Phys. Rev. B* **52,** 4740–4743 (1995).
18. Jehl, X., Payet-Burin, P., Baraduc, C., Calemczuk, R. & Sanquer, M. Superconducting quantum interference device based resistance bridge for shot noise measurement on low impedance samples. *Rev. Sci. Instrum.* **70,** 2711–2714 (1999).
19. Deutscher, G. & de Gennes, P. G. in *Superconductivity* (ed. Parks, R. D.) 1005–1034 (Dekker, New York, 1969).
20. Courtois, H., Charlat, P., Gandit, Ph., Mailly, D. & Pannetier, B. The spectral conductance of a proximity superconductor and the re-entrance effect. *J. Low Temp. Phys.* **116,** 187–214 (1999).
21. Petrashov, V. T., Shaikhaidarov, R. Sh., Delsing, P. & Claeson, T. Phase-sensitive reentrance into the normal state of mesoscopic SNS structures. *JETP Lett.* **67,** 513–520 (1998).
22. Artemenko, S. N., Volkov, A. F. & Zaitsev, A. V. On the excess current in microbridges S-c-S and S-c-N. *Solid State Commun.* **30,** 771–773 (1979).
23. Pothier, H., Guéron, S., Birge, N. O., Esteve, D. & Devoret, M. H. Energy distribution function of quasiparticles in mesoscopic wires. *Phys. Rev. Lett.* **79,** 3490–3493 (1997).
24. Altshuler, B. L. & Aronov, A. G. in *Electron-Electron Interaction in Disordered Systems* (eds Efros, A. L. & Pollak, M.) 1–153 North-Holland, Amsterdam, 1985).
25. Altshuler, B. L., Aronov, A. G., Gershenson, M. E. & Sharvin, Yu. V. Quantum effects in disordered metal films. *Sov. Sci. A* **9,** 223–354 (1987).
26. Martin, T. Wave packet approach to noise in N-S junctions. *Phys. Lett. A* **220,** 137–142 (1996).
27. Anantram, M. P. & Datta, S. Current fluctuations in mesoscopic systems with Andreev scattering. *Phys. Rev. B* **53,** 16390–16402 (1996).
28. Gramespacher, T. & Büttiker, M. Distribution functions and current-correlations in normal-metal-superconductor hetero-structures. *Phys. Rev. B* **61,** 8125 (2000).
29. Torrès, J. & Martin, T. Positive and negative Hanbury-Brown and Twiss correlations in normal metal-superconducting devices. Preprint cond-mat/9906012 at ⟨http://xxx.lanl.gov⟩ (1999).
30. Lesovik, B. G., Martin, T. & Torrès, J. Josephson frequency singularity in the noise of normal metal-superconductor junctions. *Phys. Rev. B* **60,** 11935–11938 (1999).
31. Kozhevnikov, A. A., Schoelkopf, R. J., Calvet, L. E., Prober, D. E. & Rooks, M. J. Shot noise measurements in diffusive normal-metal-superconductor (N–S) junctions. *J. Low Temp. Phys.* **118,** 671–678 (2000).

Correspondence and requests for materials should be addressed to M.S. (e-mail: msanquer@cea.fr).

Elastic turbulence in a polymer solution flow

A. Groisman & V. Steinberg

Department of Physics of Complex Systems, Weizmann Institute of Science, Rehovot 76100, Israel

Turbulence is a ubiquitous phenomenon that is not fully understood. It is known that the flow of a simple, newtonian fluid is likely to be turbulent when the Reynolds number is large (typically when the velocity is high, the viscosity is low and the size of the tank is large[1,2]). In contrast, viscoelastic fluids[3] such as solutions of flexible long-chain polymers have nonlinear mechanical properties and therefore may be expected to behave differently. Here we observe experimentally that the flow of a sufficiently elastic polymer solution can become irregular even at low velocity, high viscosity and in a small tank. The fluid motion is excited in a broad range of spatial and temporal scales, and we observe an increase in the flow resistance by a factor of about twenty. Although the Reynolds number may be arbitrarily low, the observed flow has all the main features of developed turbulence. A comparable state of turbulent flow for a newtonian fluid in a pipe would have a Reynolds number as high as 10^5 (refs 1, 2). The low Reynolds number or 'elastic' turbulence that we observe is accompanied by significant stretching of the polymer molecules, resulting in an increase in the elastic stresses of up to two orders of magnitude.

Motion of simple, low molecular weight, newtonian fluids is governed by the Navier–Stokes equation[1,2]. This equation has a nonlinear term, which is due to fluid inertia. The ratio between the nonlinearity and viscous dissipation is given by the Reynolds number, $\mathrm{Re} = VL/\nu$, where V is velocity, L is characteristic size and ν is kinematic viscosity of the fluid. When Re is high, nonlinear effects are strong and the flow is likely to be turbulent; therefore, turbulence is a paradigm for a strongly nonlinear phenomenon[1,2].

Solutions of flexible high molecular weight polymers differ from newtonian fluids in many aspects[3]. The most notable elastic property of the polymer solutions is that stress does not immediately become zero when the fluid motion stops, but rather decays with some characteristic time, λ, which can reach seconds and even minutes. The equation of motion for dilute polymer solutions differs from the Navier–Stokes equation by an additional linear term arising from the elastic stress, τ (ref. 3). Because the elastic stress is caused by stretching of the polymer coils, it depends on history of motion and deformation of fluid elements along their flow trajectories. This implies a nonlinear relationship between τ and the rate of deformation in a flow[3]. The nonlinear mechanical properties of polymer solutions are well manifested in their large extensional viscosity at high rates of extension[4] and in the Weissenberg effect[3,5]. The degree of nonlinearity in the mechanical properties is expressed by the Weissenberg number, $\mathrm{Wi} = V\lambda/L$, which is a product of characteristic rate of deformation and the relaxation time, λ.

We considered whether the nonlinearity of mechanical properties of a fluid can give rise to turbulent flow when the equation of motion is linear. For a polymer solution this corresponds to a state in which the Weissenberg number is large, while the Reynolds number is small. This situation can be realized if the parameter of

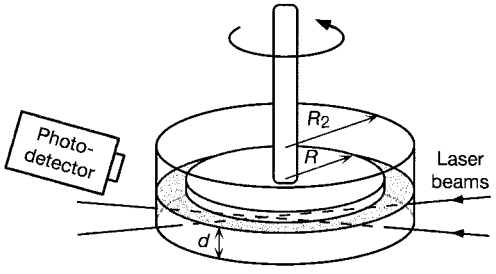

Figure 1 The experimental set-up. A stationary cylindrical cup with a plain bottom (the lower plate) is concentric with the rotating upper plate, which is attached to the shaft of a commercial rheometer. The radii of the upper and the lower plates are $R = 38$ mm and $R_2 = 43.6$ mm, respectively. The liquid is filled until a level d of 10 mm unless otherwise stated. The upper plate just touches the surface of the liquid. A special cover is used to minimize evaporation of the liquid. We used a solution of 65% saccharose and 1% NaCl in water, viscosity $\eta_s = 0.324$ Pa s, as a solvent for the polymer. We added polyacrylamide ($M_w = 18{,}000{,}000$; Polysciences) at a concentration of 80 p.p.m. by weight. The solution viscosity was $\eta = 0.424$ Pa s at $\dot{\gamma} = 1\ \mathrm{s}^{-1}$. The relaxation time, λ, estimated from the phase shift between the stress and the shear rate in oscillatory tests, was 3.4 s. The temperature is stabilized at 12 °C by circulating water under the steel lower plate. The walls of the cup are transparent which allows Doppler velocimeter measurements by collecting light scattered from the crossing point of two horizontal laser beams. In experiments where the flow has to be viewed from below, the lower plate is made from plexiglass and a mirror tilted by 45° is placed under the lower plate. The flow patterns are then captured by a CCD camera at the side and the temperature is stabilized by circulating air in a closed box.

© 2000 Macmillan Magazines Ltd

elasticity, $\mathrm{Wi/Re} = \lambda\nu/L^2$, is large enough. An important observation concerning the influence of the nonlinear mechanical properties on flow was made about a decade ago, when purely elastic instability was experimentally identified in curvilinear shear flows[6,7]. This instability occurs at moderate Wi and vanishingly small Re and is driven by the elastic stresses[7,9]. As a result of the instability, secondary and in general oscillatory vortex flows develop, and flow resistance increases[6–10]. Flow instabilities in elastic liquids are reviewed in refs 11, 12.

There is no commonly accepted unique definition of turbulent flow[2], and it is usually identified by its main features[1,2]. Turbulence implies fluid motion in a broad range of spatial and temporal scales, so that many degrees of freedom are excited in the system. A practically important characteristic of turbulent flows is a large increase in the flow resistance compared with an imaginary laminar flow with the same Re. We show how these main features of turbulence appear in a flow of a highly elastic polymer solution at low Reynolds numbers.

For our experiments we chose a swirling flow between two parallel disks (Fig. 1), and a dilute solution of high molecular weight polyacrylamide in a viscous sugar syrup as the working fluid. The curvature ratio was made quite high, $d/R = 0.263$, to provide destabilization of the primary shear flow and development of the secondary vortical fluid motion at lower shear rates[7,10]. (The flow between two plates with small d/R has been studied previously in the context of the purely elastic instability[10].) We mounted the whole flow set-up on top of a commercial viscometer (AR-1000 of TA-instruments) to measure precisely the angular velocity, ω, of the rotating upper plate and the torque applied to it. In this way we were able to estimate the average shear stress, σ, in the polymer solution and to compare it with the stress in the laminar flow, σ_{lam}, with the same applied shear rate. In newtonian fluids the ratio $\sigma/\sigma_{\mathrm{lam}}$ generally grows with Re as the flow becomes increasingly irregular, and the magnitude of $\sigma/\sigma_{\mathrm{lam}}$ can be considered as a measure of strength of turbulence and turbulent resistance. In our set-up σ becomes 30% higher than σ_{lam} at $\mathrm{Re} = 70$, which can be regarded as a point when inertial effects become significant.

The dependence of $\sigma/\sigma_{\mathrm{lam}}$ on the shear rate, $\dot{\gamma} = \omega R/d$, for flow of the polymer solution in the experimental system is shown in Fig. 2 (first curve). At a value of $\dot{\gamma}$ of about $1\,\mathrm{s}^{-1}$ (corresponding to $\mathrm{Wi} \equiv \lambda\dot{\gamma} = 3.5$), a sharp transition occurs that appears as a significant increase in the apparent viscosity. The Reynolds number at the transition point is about 0.3, which means that the inertial effects are quite negligible. The transition has pronounced hysteresis,

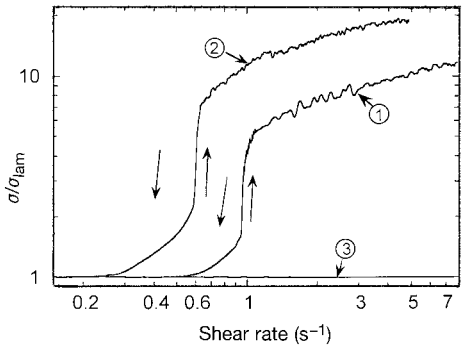

Figure 2 Stress ratio versus shear rate. We plot the ratio of the average stress, σ, measured in the flow, to the stress, σ_{lam}, in the laminar flow with the same boundary conditions as a function of the shear rate, $\dot{\gamma}$. The curves 1 and 2 are for the polymer solution flow with $d = 10$ mm and 20 mm, respectively. The shear rate was gradually varied in time, very slowly (by about 10% h^{-1}) in the transition region, and faster below and above it. Thin black lines represent increasing $\dot{\gamma}$; thick grey lines represent decreasing $\dot{\gamma}$. Curve 3 represents the pure solvent. Mechanical degradation of the polymers was quite small at shear rates below $1.5\,\mathrm{s}^{-1}$ and $1\,\mathrm{s}^{-1}$ for $d = 10$ mm and 20 mm, respectively. The dependences of $\sigma/\sigma_{\mathrm{lam}}$ on $\dot{\gamma}$ in those regions were therefore reproducible in consecutive runs within about 1%. Degradation effects became appreciable at higher shear rates, and elasticity typically decreased by up to 10% as a result of the runs shown by the curves 1 and 2.

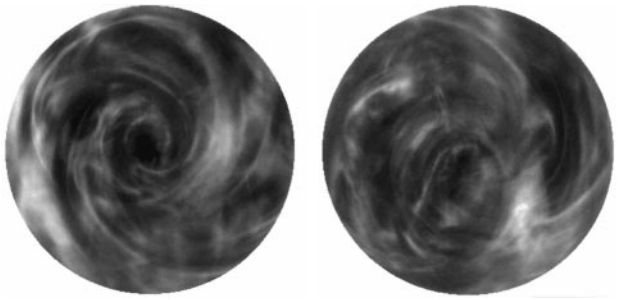

Figure 3 Two snapshots of the flow at $\mathrm{Wi} = 13$, $\mathrm{Re} = 0.7$. The flow under the black upper plate is visualized by seeding the fluid with light reflecting flakes (1% of the Kalliroscope liquid). The fluid is illuminated by ambient light. Although the pattern is quite irregular, structures that appear tend to have spiral-like forms. The dark spot in the middle corresponds to the centre of a big persistent thoroidal vortex that has dimensions of the whole set-up.

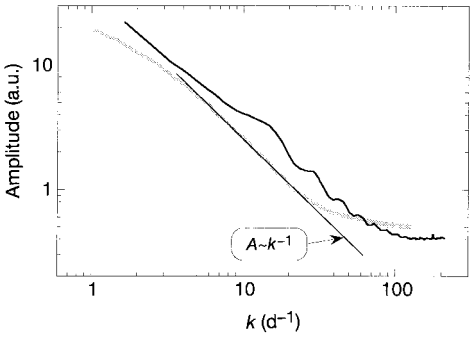

Figure 4 Average Fourier spectra of the brightness profiles. These are taken along the diameter (thin black line) and along the circumference at a radius of $2d$ (thick grey line). We averaged over a long series of flow pattern snapshots taken in consecutive moments of time. The wavelength is measured in units of d, so that the wavenumber, k, of unity corresponds to a length of $2\pi d$. The spectrum taken along the diameter apparently differs from the azimuthal spectrum by a series of broad peaks. This may be a manifestation of the fact that the flow is not completely structureless and homogeneous along the radial direction (see Fig. 3). The visualization method that we used (Fig. 3) does not provide direct information about the fluid velocity; therefore, the exact value of the exponent in the power law fit, $A \approx K^{-1}$, has no special meaning.

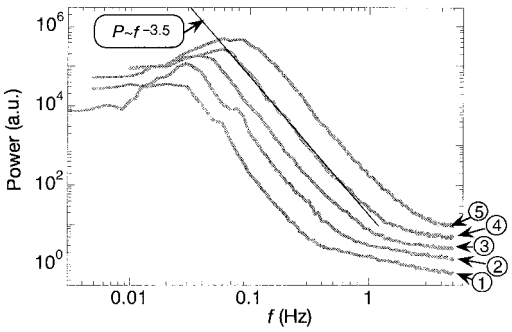

Figure 5 Power spectra of velocity fluctuations. The data are obtained at different rates, $\dot{\gamma}$ in the standard set-up. The fluid velocity was measured by a laser Doppler velocimeter in the centre of the flow. Curves 1–5 correspond to $\dot{\gamma} = 1.25$, 1.85, 2.7, 4 and $5.9\,\mathrm{s}^{-1}$, respectively (all above the transition point $\dot{\gamma} \simeq 1$, Fig. 2). The power, P, of fluctuations is fitted by a power law, $P \approx f^{-3.5}$, for $\dot{\gamma} = 4\,\mathrm{s}^{-1}$ over about a decade in frequencies, f.

© 2000 Macmillan Magazines Ltd

which is typical for the purely elastic flow instability[9]. The ratio σ/σ_{lam} keeps growing with the shear rate, and at the highest $\dot{\gamma}$ that has been reached the flow resistance is about 12 times larger than is found in laminar flow. In the same range of shear rates, flow of the pure solvent is completely laminar and the ratio σ/σ_{lam} is unity within the resolution of the viscometer (about 1%). To make sure that the observed flow phenomena were indeed caused by the solution elasticity, we measured σ for a few solutions that had the same polymer concentration but different relaxation times, λ. The curves of σ/σ_{lam} coincided, when plotted against Wi, whereas the Reynolds number turned out to be completely irrelevant (see also ref. 9). The growth of the resistance in the polymer solution flow becomes even larger when the size of the gap is increased (Fig. 2, second curve). At this point the ratio σ/σ_{lam} reaches a value of 19. Such growth of the flow resistance is found for newtonian fluids in the same flow geometry at Re of about 2×10^4. For flow in a circular pipe this value of σ/σ_{lam} is reached at $Re \simeq 10^5$, which is usually considered as a region of rather developed turbulence[1].

Two representative snapshots of the polymer solution flow above the transition (at $\dot{\gamma} = 4\,s^{-1}$) are shown in Fig. 3. The flow patterns are very irregular and structures of different sizes appear. This visual impression is confirmed by a more careful analysis. Average Fourier spectra of the brightness profiles along the diameter and along the circumference exhibit power law decay over a decade in the wavenumber domain (Fig. 4).

Characteristic time spectra of velocity fluctuations at different shear rates are shown in Fig. 5. Flow velocity was measured in the horizontal plane in the centre of the set-up, where its average value is zero. As the shear rate is raised the power of fluctuations increases and characteristic frequencies become higher, but the general form of the spectra remains very much the same. In particular, just as for the spatial spectra in Fig. 4, there is a region of a power law decay, which spans about a decade in frequencies. This power law dependence in the broad ranges of spatial and temporal frequencies actually means that the fluid motion is excited at all those spatial and temporal scales. Spectra of radial and azimuthal velocities taken at different points with non-zero average flow had the same general appearance and close values of exponents in the power law decay range.

In summary, we conclude that the flow of the elastic polymer solution at sufficiently high Wi has all the main features of developed turbulence. By the strength of the turbulent resistance, and by the span of scales in space and time, where the fluid motion is excited, the observed flow can be compared with turbulence in a newtonian fluid in a pipe at Re of about 10^5. This apparently turbulent flow arises solely because of the nonlinear mechanical properties of the elastic polymer solution. We therefore call the phenomenon elastic turbulence, in contrast to the usual inertial turbulence which is observed in newtonian fluids at high Re. (The name 'elastic turbulence' has been used before for designation of apparently disordered flows in polymeric liquids[13]. No attempt has been ever made, however, to characterize those flows quantitatively.)

Elastic turbulence has many features that are in sharp contradiction to the concepts of newtonian fluid mechanics. On the one hand, velocity required for excitation of inertial turbulence in a newtonian fluid is proportional to the fluid viscosity. On the other hand, the polymer relaxation time, λ, usually grows proportionally to the viscosity. Because at constant d/R the transition to elastic turbulence occurs at a certain value of the Weissenberg number, $Wi = V\lambda/L$, one can excite turbulence at lower velocities by choosing more viscous polymer solutions. Indeed, using a solution of polymers in a very viscous sugar syrup, we observed transition to the elastic turbulence at a rotation rate of $0.05\,s^{-1}$ (corresponding to $Re \simeq 10^{-3}$). Further, in an elastic polymer solution, the scale of time, λ, does not depend on the size of the system; therefore as long as the ratio d/R is preserved, transition to turbulence should occur at the same ω, and the dependence of σ/σ_{lam} on $\dot{\gamma}$ should not change with the size of the system. We repeated the measurements of σ in a small set-up having all the dimensions reduced by a factor of 4 as compared with the standard system. The dependence of σ/σ_{lam} on $\dot{\gamma}$ was found to be the same (data not shown) as in Fig. 2, whereas the characteristic velocities and the Reynolds numbers were lower by factors of 4 and 16, respectively. We therefore believe that by using polymer solutions with sufficiently high elasticity we can excite turbulent motion at arbitrary low velocities and in arbitrary small tanks. (The size of the tank still has to be large compared with the size of the polymer coils.)

An important question about the elastic turbulence is where the turbulent resistance comes from. In the inertial turbulence the origin of the large resistance is the Reynolds stress, which is connected with high kinetic energy of the turbulent motion and takes a major part in the momentum transfer in the flow. Elastic turbulence occurs at low Reynolds numbers. From our velocity measurements in the standard set-up, contribution of the Reynolds stress to the flow resistance could be estimated as being less than 0.5%. The contribution of the viscous shear stress of the newtonian solvent, averaged across the fluid layer, is always the same as in laminar flow and cannot change. Thus, the whole increase in the flow resistance should be due to the elastic stress. The data shown in Fig. 2 (second curve) imply that the polymer contribution to the stress increases by a factor of up to 65, as compared with laminar flow with the same average shear rate. This suggestion agrees very well with our measurements of relaxation of the shear stress after the fluid motion is stopped. The elastic part, τ, of the whole stress is identified by its slow relaxation with a characteristic time of the order λ. In elastic turbulence this slowly relaxing part can become two orders of magnitude larger than in laminar flow with the same shear rate. This major growth of the elastic stress should be connected with vast extension of the polymer molecules in the turbulent flow.

Thus, elastic turbulence apparently develops as follows. The polymer molecules are stretched in the primary shear flow, which makes it unstable and causes irregular secondary flow. This flow acts back on the polymer molecules, stretching them further and becoming increasingly turbulent, until a kind of saturated dynamic state is reached. The density of the elastic energy of the stretched polymers can be estimated as $Wi\,\tau/2$, and should therefore increase in the elastic turbulent flow by about the same factor as the elastic stress, τ, while the kinetic energy remains small. □

Received 6 December 1999; accepted 2 March 2000.

1. Landau, L. D. & Lifschitz, E. M. *Fluid Mechanics* (Pergamon, Oxford, 1987).
2. Tritton, D. J. *Physical Fluid Dynamics* (Clarendon, Oxford, 1988).
3. Bird, R. B., Curtiss, C. F., Armstrong, R. C. & Hassager, O. *Dynamics of Polymeric Liquids* (Wiley, New York, 1987).
4. Tirtaatmadja, V. & Sridhar, T. A filament stretching device for measurement of extensional viscosity. *J. Rheology* **37,** 1081–1102 (1993).
5. Weissenberg, K. A continuum theory of rheological phenomena. *Nature* **159,** 310–311 (1947).
6. Magda, J. J. & Larson, R. G. A transition occuring in ideal elastic liquids during shear flow. *J. Non-Newtonian Fluid Mech.* **30,** 1–19 (1988).
7. Muller, S. J., Larson, R. G. & Shaqfeh, E. S. G. A purely elastic transition in Taylor–Couette flow. *Rheol. Acta* **28,** 499–503 (1989).
8. Larson, R. G., Shaqfeh, E. S. G. & Muller, S. J. A purely viscoelastic instability in Taylor–Couette flow. *J. Fluid Mech.* **218,** 573–600 (1990).
9. Groisman, A. & Steinberg, V. Mechanism of elastic instability in Couette flow of polymer solutions: experiment. *Phys. Fluids* **10,** 2451–2463 (1998).
10. Byars, J. A., Öztekin, A., Brown, R. A. & McKinley, G. H. Spiral instabilities in the flow of highly elastic fluids between rotating parallel disks. *J. Fluid Mech.* **271,** 173–218 (1994).
11. Larson, R. G. Instabilities in viscoelastic flows. *Rheol. Acta* **31,** 213–263 (1992).
12. Shaqfeh, E. S. G. Purely elastic instabilities in viscometric flows. *Annu. Rev. Fluid. Mech.* **28,** 129–185 (1996).
13. Giesekus, H. W. Non-linear effects in the flow of visco-elastic fluids through slits and holes. *Rheol. Acta* **7,** 127–138 (1968).

Acknowledgements

This work was supported by the Minerva Center for Nonlinear Physics of Complex Systems.

Correspondence and requests for materials should be addressed to A. G.

© 2000 Macmillan Magazines Ltd